

Clinical and Immune Features of Pneumocystis Pneumonia with Acute Respiratory Distress Syndrome in Immunocompromised Children

DongDong Feng¹, Chao Chen², HuiMin Huang², and XueQiong Huang²

¹ Department of Pediatrics, Guangxi Hospital Division of The First Affiliated Hospital, Sun Yat-sen University, Nanning, Guangxi Zhuang Autonomous Region, China

² Pediatric Intensive Care Unit (PICU), The First Affiliated Hospital, Sun Yat-sen University, Guangzhou, China

Received: 4 July 2025; Received in revised form: 4 October 2025; Accepted: 27 October 2025

ABSTRACT

Pneumocystis jirovecii pneumonia (PJP) is a common opportunistic infection in immunocompromised children, often causing acute fulminant pneumonia with respiratory failure. The prognosis of PJP in human immunodeficiency virus (HIV)-negative children with acute respiratory distress syndrome (ARDS) remains unclear.

This retrospective review (2015–2021) included 20 HIV-negative children with ARDS and PJP. Among them, 17 had hematological malignancies or solid tumors, and 3 had renal disease; 15 survived, 5 did not. Both groups had very low CD4⁺ T cell counts ($<0.2 \times 10^9/L$), severe ARDS (partial pressure of oxygen in arterial blood / fraction of inspired oxygen [PaO₂/FiO₂] ratio <150), and elevated lactate dehydrogenase (LDH) and (1,3)- β -D-glucan (BDG) levels. In non-survivors, anti-PJP therapy was initiated approximately 7 days later than in survivors.

Single-cell sequencing revealed CD4⁺/CD8⁺ T cell ratios of 0.16 (survivors) vs 2.13 non-survivors), with a higher ratio of regulatory T cells (Tregs) to CD4⁺ T cells in non-survivors (33% vs. 10.6%). Non-survivors showed enrichment of neutrophil degranulation and activation pathways and expressed more proapoptotic and proinflammatory signals (e.g., *FAS*, *FASLG*, interferon- γ).

Early treatment initiation is critical. Prolonged CD8⁺ T cell deficiency, high Treg expression with proapoptotic genes, and excessive inflammation may predict poor prognosis.

Keywords: Acute; Immunocompromised host; *Pneumonia*, *Pneumocystis*; Respiratory distress syndrome; Regulatory T-lymphocytes; T-lymphocytes

INTRODUCTION

Pneumocystis jirovecii pneumonia (PJP) was first identified as an opportunistic pathogen in patients with

human immunodeficiency virus (HIV) infection.¹ With the application of immunosuppressants, antitumor chemotherapies, and transplantation in recent years, the incidence of PJP in immunosuppressed individuals without HIV infection should not be underestimated.^{2,3} In addition, acute respiratory distress syndrome (ARDS) secondary to PJP develops rapidly and is severe, which often requires an intensive care unit (ICU) stay for invasive ventilator-assisted ventilation and has a high

Corresponding Author: XueQiong Huang, PhD;
Pediatric Intensive Care Unit (PICU), The First Affiliated Hospital,
Sun Yat-sen University, Guangzhou, China. Tel: (+86 136) 0247 6465,
Fax: (+86 020) 3659 5510, Email Huangxq9@mail.sysu.edu.cn
*The first and second authors contributed equally to this study

mortality rate.^{4,5} Establishing the diagnosis of PJP is difficult because of the lack of a reliable culture system. Although cysts can be stained with Grocott–Gomori methenamine silver (GMS), which has good specificity, its sensitivity is not satisfactory. However, the development of polymerase chain reaction (PCR) and metagenomic next-generation sequencing (mNGS) pathogen detection technology has greatly improved the detection rate of cysts and specificity and is highly valuable in the diagnosis of PJP.^{6,7}

The severity of PJP in HIV-negative patients is greater than that in HIV-associated PJP, with a more rapid and fulminant onset, and the mortality rate associated with PJP in HIV-negative patients is approximately 30% to 60%.^{8,9} The 90-day mortality rate of patients with severe PJP who required high-flow nasal oxygen (HFNO) with at least 50% fraction of inspired oxygen (FiO₂), noninvasive ventilation, or mechanical ventilation increased to 50%.¹⁰

We retrospectively analyzed the clinical and immune data of immunocompromised children with ARDS secondary to PJP in our hospital and aimed to compare the differences between survivors and non-survivors. We aimed to identify the molecular biomarkers and pathways that could be therapeutically controlled to improve the PJP with ARDS trajectory toward better outcomes by tracking temporal expression changes in specific cell types, which could lead to more accurate predictions.

MATERIALS AND METHODS

We retrospectively analyzed children with ARDS secondary to PJP diagnosed in an 8-bed pediatric ICU (PICU) of our hospital from May 2015 to January 2021. The requirement for informed consent was waived owing to the retrospective nature of this study.

Study Population

All children aged younger than 18 years were screened for inclusion in this study. The diagnosis of ARDS was based on the need for invasive or noninvasive ventilation. The diagnosis of PJP was established based on the presence of lesions on chest radiography or computed tomography (CT) and the detection and identification of pathogens. Pathogens were detected by high-throughput sequencing using the Illumina HiSeq platform (Illumina, Inc., USA) on obtained bronchoalveolar lavage fluid (BALF) or blood

specimens. Simultaneously, hexamine silver dye (Grocott's methenamine silver stain kit, Sigma-Aldrich, USA) was sent for microbial identification of *Pneumocystis jirovecii*.

Inclusion Criteria

Patients were included if they met all of the following criteria:

1. Aged <18 years.
2. Met the diagnostic criteria for ARDS, based on the need for invasive or noninvasive ventilatory support.
3. Had a confirmed diagnosis of PJP, established by both:

Radiographic evidence: Presence of suggestive lesions on chest radiography or high-resolution computed tomography (CT).

Microbiological confirmation: Detection of *Pneumocystis jirovecii* through high-throughput sequencing of bronchoalveolar lavage fluid (BALF) or blood specimens, supplemented by hexamine silver staining for microbial identification.

Exclusion Criteria

Patients were excluded if they met any of the following criteria:

1. HIV Infection: Confirmed human immunodeficiency virus (HIV) infection.
2. Co-infection with confounding pathogens: Concurrent active infection with other major pathogens at the time of PJP diagnosis that could independently lead to ARDS or confound PJP-specific outcomes, including infections that require specific treatment, such as microbiologically confirmed invasive aspergillosis or cytomegalovirus disease requiring antiviral therapy.
3. Insufficient Data: Incomplete medical records or missing key clinical/laboratory data essential for analysis.
4. Lost to Follow-up: Transfer to another hospital within 48 hours of Pediatric Intensive Care Unit (PICU) admission, preventing assessment of primary outcomes.

Data Collection

The following ICU admission data were extracted from the medical records: general demographic information, underlying disease, medications in the preceding months, PJP prophylaxis, duration of dyspnea before admission, renal replacement therapy (RRT), vasoactive drug support, anti-PJP drugs, and emerging organ failure during ICU hospitalization. The Pediatric

PJP-ARDS in Immunocompromised Children

Critical Care Score and Pediatric Risk of Mortality Score were used to assess disease severity. In addition, mechanical ventilation support parameters (peak inspiratory pressure [PIP] and positive end-expiratory pressure [PEEP]) and laboratory data, including alveolar-arterial oxygen gradient, partial pressure of oxygen (PaO₂)/FiO₂ ratio (P/F ratio), C-reactive protein (CRP) and procalcitonin (PCT) levels, white blood cell count (WBC), neutrophil-to-lymphocyte ratio (NLR), and (1,3)-β-D-glucan level measured by the Fungitell assay (Primerdesign, UK) and Cryptococcus and *Aspergillus* antigen test (Cryptococcal antigen lateral flow assay, Immuno-Mycologics, USA), were collected. Finally, length of ICU stay, length of hospital stay, and hospital mortality were recorded.

To determine the immune differences in peripheral blood T lymphocytes between survivors and non-survivors, we performed single-cell sequencing of peripheral blood from survivors and non-survivors on day 5 after the diagnosis of PJP-associated ARDS was established, using the 10x Genomics Chromium platform (USA).

Functional Enrichment Analysis of the Differential Genes Using the Gene Ontology

We first used the FindMarker function to identify the respective upregulated genes in the subsets of CD4⁺ T and CD8⁺ T cells and retained only genes with a log₂ fold change (log₂fc) >0.25, with *p*<.05 considered significant.

Gene Set Variation and Gene Set Enrichment Analyses

Gene set variation analysis (GSVA) is a nonparametric, unsupervised algorithm. Differential expression analysis of the gene set for signaling pathways was performed using GSVA (GSVA R package, USA). Gene set enrichment analysis (GSEA) was used to compare the enrichment analysis of gene sets in subsets of identical cells derived from different groups of samples (GSEA software, USA).

Cell Communication Analysis

Cell communication analysis focuses on RNA expression, applies the CellPhoneDB algorithm and database (CellPhoneDB v2.0, UK) to obtain the expression information of the ligand–receptor gene of cells, calculates the co-expression relationship of ligand

receptors between cells, and obtains the signal communication relationship between cell subsets.

Statistical Analyses

Continuous data are presented as mean ± standard deviation (SD), whereas categorical data are presented as numbers and percentages (%). Means between groups were compared using *t* test or Mann–Whitney *U* test (if normality was not assumed). Categorical data were tested using the chi-squared test or Fisher's exact test. Statistical significance was set at *p*<.05, two-tailed. All analyses were performed using the International Business Machines (IBM) Statistical Package for the Social Sciences (SPSS) version 25 (SPSS Statistics version 25, IBM Corporation, Armonk, NY, USA).

RESULTS

Patients' Clinical Characteristics

Twenty patients were included in this study. The mean age of all patients was 6.34 ± 3.57 years, and the sex ratio (male:female) was 8:12. There were 15 and 5 patients with survival and non-survival outcomes, respectively. Seventeen patients had underlying malignancies (10 hematological malignancies, 7 solid tumors), and the other 3 had renal disease. The baseline characteristics of the survival and non-survival groups are shown in Table 1. The medication usage of survivors and non-survivors can be found in Supplementary Table S1. Regarding anti-PJP therapy, trimethoprim-sulfamethoxazole (TMP-SMX) was administered to 16 patients (13 survivors, 3 non-survivors), while pentamidine was used in 4 patients (2 survivors, 2 non-survivors) due to TMP-SMX intolerance. Adjunctive corticosteroids were administered to 18 patients (14 survivors, 4 non-survivors) as part of the standard management for severe PJP with ARDS. As indicated, the duration of dyspnea before anti-PJP therapy, duration of respiratory support, and length of stay were significantly longer in the non-survival group than in the survival group (*p*<.05). The initiation of anti-PJP therapy was later in the non-survival group (*p*<.05).

Table 1. Patients' clinical characteristics between groups

Variable	Survival group (n=15)	Non-survival group (n=5)	All (n=20)	p
Age, y	6.01 ± 3.00	7.32 ± 5.23	6.34 ± 3.57	0.494
Body weight, kg	20.56 ± 9.18	23.70 ± 15.41	21.35 ± 10.68	0.583
Duration of dyspnea before anti-PJP, d	1.97 ± 1.17	7.20 ± 2.68	3.28 ± 2.82	<0.001
Duration of underlying disease, mo	10.30 ± 11.96	14.40 ± 12.46	11.33 ± 11.89	0.519
Duration of ICU stay, d	11.07 ± 5.23	19.00 ± 3.08	13.05 ± 5.88	0.005
Time to anti-PJP therapy, d	3.30 ± 1.36	10.80 ± 4.49	5.18 ± 4.09	<0.001
PRISM	13.40 ± 3.62	14.00 ± 3.39	13.55 ± 3.49	0.749
Male:female	5:10	3:2	8:12	0.314
Underlying disease				
Leukemia	5 (33%)	2 (40%)	7 (35%)	NA
Lymphoma	3 (20%)	0	3 (15%)	NA
Solid tumor	5 (33%)	2 (40%)	7 (35%)	NA
Immune and kidney diseases	2 (13%)	1 (20%)	3 (15%)	NA
Anti-PJP				
TMP-SMX/(TMP-SMX + caspofungin)	5/10	1/4	6/14	>0.99
Primary disease treatment stage				
Corticosteroid + immunosuppressant	2 (13%)	2 (40%)	4 (20%)	NA
Consolidation chemotherapy	7 (47%)	1 (20%)	8 (40%)	NA
Continuous chemotherapy	2 (13%)	2 (40%)	4 (20%)	NA
Induction chemotherapy	4 (27%)	0	4 (20%)	NA
Myelosuppression	8 (53%)	3 (60%)	11 (55%)	>0.99
AKI	1 (7%)	2 (40%)	3 (15%)	0.140
Mediastinal emphysema	1 (7%)	1 (20%)	2 (10%)	0.447
Abnormal cardiac function	1 (7%)	2 (40%)	3 (15%)	0.140
EBV/CMV infection	0	2 (40%)	2 (10%)	0.053
<i>Streptococcus pneumoniae</i>	2 (13%)	1 (20%)	3 (15%)	>0.99
<i>Aspergillus</i>	0	1 (20%)	1 (5%)	0.250
VAP	2 (13%)	0	2 (10%)	>0.99
mNGS				
Blood	1 (7%)	2 (40%)	3 (15%)	NA
BALF	14 (93%)	3 (60%)	17 (85%)	NA
Respiratory support (IMV/NIV)	14/1	5/0	19/1	0.222
NIV for weaning	6/14	0	6/14	NA
Fluid balance (in a week), mL/kg·d	5.79 ± 12.47	3.11 ± 8.09	5.12 ± 11.39	0.660
Corticosteroid treatment	12 (80%)	3 (60%)	15 (75%)	0.560

^aData are reported as the mean ± standard deviation, median (interquartile range), or count (%), as appropriate for the data type.

^bAKI: acute kidney injury; BALF: bronchoalveolar lavage fluid; CMV: cytomegalovirus; EBV: Epstein-Barr virus; ICU: intensive care unit; IMV: invasive mechanical ventilation; mNGS: metagenomic next-generation sequencing; NA: not applicable; NIV: noninvasive ventilation; PRISM: Pediatric Risk of Mortality; TMP-SMX: trimethoprim-sulfamethoxazole; VAP: ventilator-associated pneumonia.

PJP-ARDS in Immunocompromised Children

Laboratory Results

Tables 2 and 3 show the laboratory results between the survival and non-survival groups. As indicated, there were no differences between the two groups on PICU admission. Both groups had severe ARDS with P/F ratio <150 and higher lactate dehydrogenase (LDH) and

(1,3)- β -D-glucan (BDG) levels. Among the indexes related to immunity, only interleukin (IL)-17 levels were higher in the non-survival group (Table 3, $p < .05$). On admission, the number of CD4⁺ T cells in both groups was lower than $0.2 \times 10^9/L$. The ratio of CD8⁺ T cells was higher than that of CD4⁺ T cells.

Table 2. Laboratory results between the survival and non-survival groups on admission

Variable	Survival group (n=15)	Non-survival group (n=5)	All (n=20)	<i>p</i>
PaO ₂ /FiO ₂ , mm Hg	121.10 ± 32.24	106.59 ± 25.67	117.47 ± 30.76	0.375
Lactate, mmol/L	0.97 ± 0.66	1.10 ± 0.45	1.00 ± 0.60	0.681
Duration of IMV/NIV, d	6.47 ± 2.53	16.60 ± 6.15	9.00 ± 5.74	<0.001
PIP, cm H ₂ O	23.79 ± 2.12	22.00 ± 2.45	23.32 ± 2.29	0.138
PEEP, cm H ₂ O	10.14 ± 2.32	10.00 ± 3.39	10.11 ± 2.54	0.918
C-reactive protein, mg/L	81.82 ± 77.77	89.79 ± 88.37	83.82 ± 78.18	0.850
Procalcitonin, ng/mL	1.31 ± 2.21	0.76 ± 0.78	1.17 ± 1.94	0.597
NT-proBNP, pg/mL	2442.69 ± 2551.59	832.00 ± 1209.24	2040.02 ± 2370.06	0.196
White blood cells, $\times 10^9/L$	5.91 ± 5.27	7.80 ± 5.60	6.38 ± 5.27	0.502
Neutrophils, $\times 10^9/L$	4.56 ± 4.36	6.82 ± 4.88	5.12 ± 4.48	0.343
Lymphocytes, $\times 10^9/L$	0.73 ± 0.76	0.57 ± 0.80	0.69 ± 0.75	0.694
APTT, s	40.89 ± 9.13	35.48 ± 12.01	39.54 ± 9.88	0.302
Creatinine, mmol/L	32.07 ± 32.50	64.60 ± 57.52	40.20 ± 41.03	0.128
LDH, U/L	821.87 ± 420.22	909.40 ± 286.04	843.75 ± 385.81	0.672
(1,3)- β -D-glucan, pg/mL	411.90 ± 227.51	360.24 ± 262.74	398.99 ± 230.65	0.676

^aData are reported as the mean ± standard deviation. ^bAPTT: activated partial thromboplastin time; FiO₂: fraction of inspired oxygen; IMV: invasive mechanical ventilation; LDH: lactate dehydrogenase; NIV: noninvasive ventilation; NT-proBNP: N-terminal pro-brain natriuretic peptide; PaO₂: partial pressure of oxygen; PEEP: positive end-expiratory pressure; PIP: peak inspiratory pressure.

Table 3. Index related to immunity between the survival and non-survival groups

Variable	Survival group (n=15)	Non-survival group (n=5)	All (n=20)	<i>p</i>
CD3 ⁺ CD4 ⁺ , %	32.57 ± 23.89	24.40 ± 6.51	30.94 ± 21.46	0.658
CD4 ⁺ T, $\times 10^9/L$	0.13 ± 0.14	0.08 ± 0.00	0.12 ± 0.12	0.658
CD3 ⁺ CD8 ⁺ , %	44.16 ± 23.66	56.15 ± 2.90	46.56 ± 21.49	0.513
CD19 ⁺ , %	11.58 ± 23.78	11.70 ± 1.20	11.59 ± 22.25	0.996
NK cell, %	7.54 ± 6.09	7.00 ± 2.55	7.43 ± 5.44	0.908
CD4 ⁺ /CD8 ⁺ ratio	1.25 ± 1.64	0.43 ± 0.09	1.08 ± 1.49	0.521
IgA, g/L	0.77 ± 0.31	1.02 ± 0.37	0.85 ± 0.33	0.320
IgM, g/L	0.30 ± 0.12	0.67 ± 0.58	0.42 ± 0.36	0.151
IgG, g/L	6.43 ± 1.52	5.06 ± 1.17	5.97 ± 1.50	0.219
IL-6, pg/mL	54.11 ± 87.23	13.82 ± 9.79	43.12 ± 75.49	0.460
IL-10, pg/mL	7.46 ± 6.58	22.05 ± 34.23	11.44 ± 17.64	0.240
TNF- α , pg/mL	1.23 ± 0.60	1.52 ± 0.87	1.31 ± 0.65	0.534
IL-17, pg/mL	2.83 ± 0.86	5.75 ± 0.81	4.00 ± 1.75	0.032

IgA: immunoglobulin A; IgG: immunoglobulin G; IgM: immunoglobulin M; IL: interleukin; NK: natural killer; TNF: tumor necrosis factor.

Radiographic Imaging in Patients with Non-Human Immunodeficiency Virus Infection

High-resolution CT of the chest most commonly demonstrates lesions dominated by lung interstitial inflammation and ground-glass opacity with relative peripheral sparing, although mosaic and diffuse patterns can be observed.^{11,12} High-resolution CT findings of PJP are shown in Figure 1.

Single-cell Sequencing Results

The results of transcriptome standard analysis using the R language Seurat package yielded 7916 and 2634 cells from two representative patients (one survivor and one non-survivor), respectively. (Table 4 and Figure 2). CD4⁺ T/CD8⁺ T cell ratios were 0.16 (337/2056) and 2.13 (595/279) in the survival and non-survival groups,

respectively, suggesting a decrease in the proportion of effector CD8⁺ T cells in non-survivors. The frequency of the CD4⁺ T cell subpopulation varied in two patients. Regulatory T cells (Tregs) are immunosuppressive and inhibit effective T cell activation and proliferation. Treg frequencies were 33% and 10.6% in the non-survival and survival groups, respectively, suggesting that the non-survival group had a higher proportion of immunosuppressive Tregs, which may weaken pathogen clearance.

The GO enrichment analyses showed that the non-survival group was dominated by neutrophil degranulation and activation (Figure 3). Degranulation from neutrophils and inflammatory reactions have been considered major causative factors of pulmonary disorders.

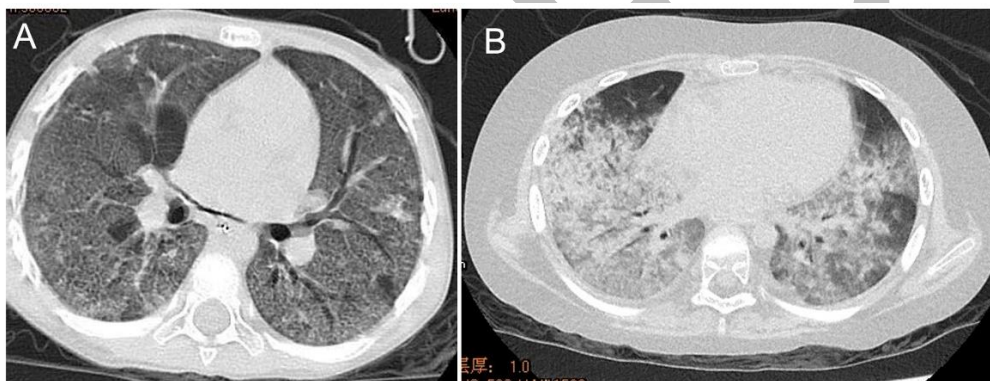
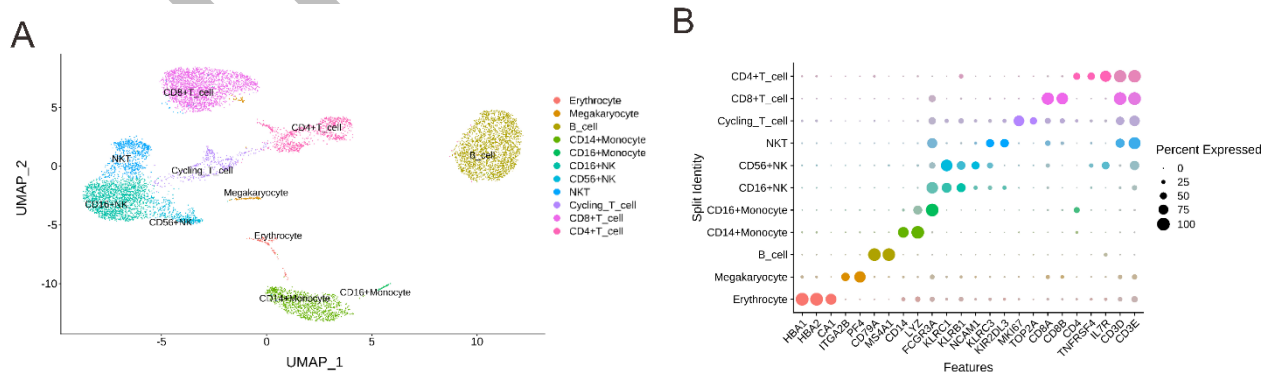


Figure 1. High-resolution chest CT image. A, Diffuse ground-glass opacity (GGO) is distributed in a panlobular manner, in which GGO with crazy paving pattern is sharply demarcated from the adjacent lung by interlobular septa. B, Extensive consolidations were in the dependent regions of both lungs, along with extensive GGO. Computed tomography changes at admission were not indicators of assessing prognosis.



PJP-ARDS in Immunocompromised Children

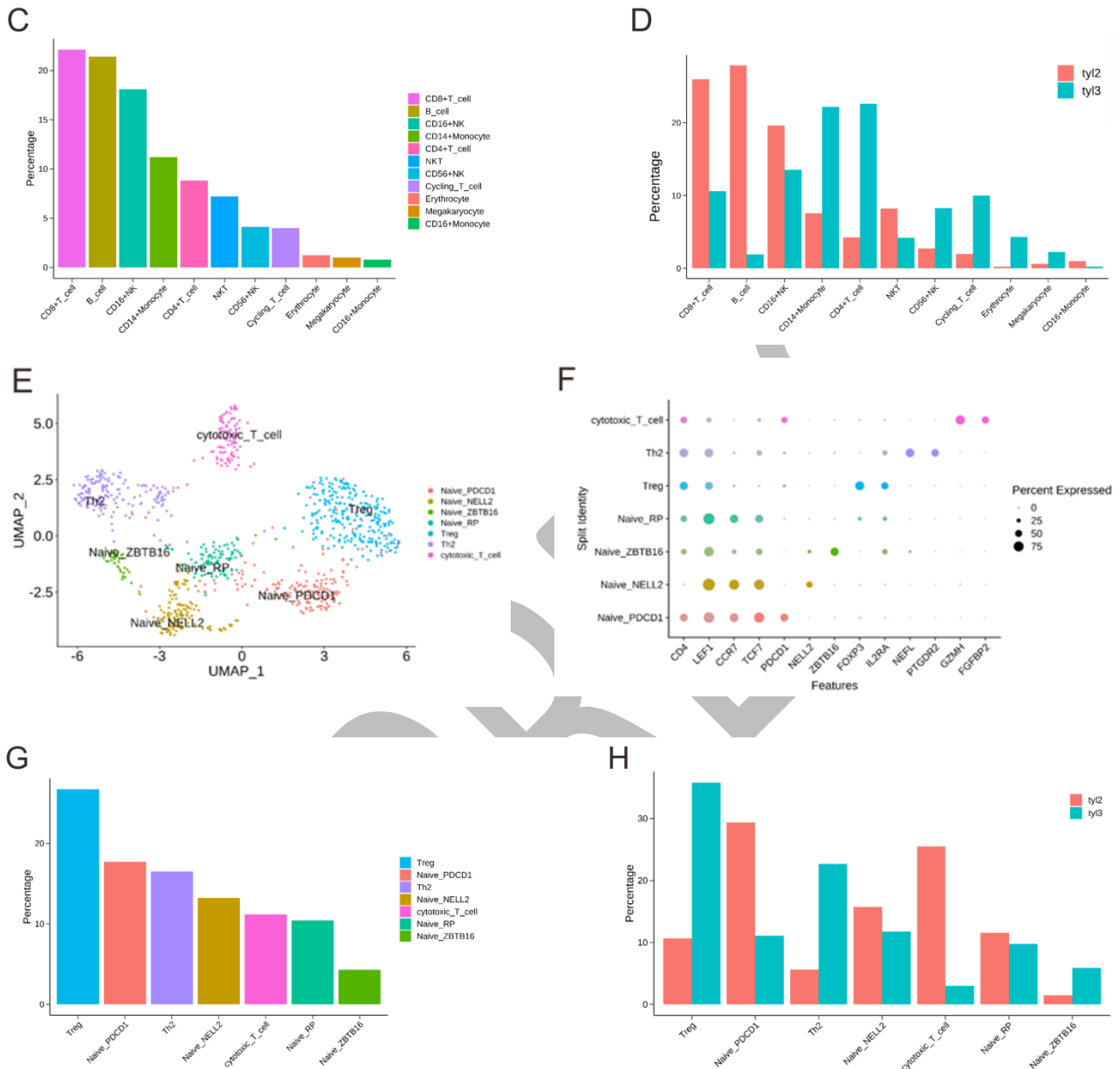


Figure 2. Analysis of immune markers in the survival and non-survival groups. **A**, Uniform Manifold Approximation and Projection (UMAP) plot showing all cells after integration and annotation based on canonical marker genes. **B**, Bubble diagrams validating the identity of major cell clusters based on the expression of key marker genes. **C**, The proportion of different cell types, CD8⁺ T cells, 22.1%; CD4⁺ T cells, 8.8%. **D**, Difference between cells in the two samples. CD4⁺ T/CD8⁺ T levels were 0.16 (337/2056) and 2.13 (595/279) in the survival and non-survival groups, respectively. This suggests a decrease in the proportion of effector T cells in non-survivors. **E**, After integration, CD8⁺ T cells were relatively unified with no evident signs of subset; CD4⁺ T cells showed clear signs of subpopulations, subdivided into seven subpopulations. Four of these subgroups belonging to the naive subset were identified by their signature genes. **F**, CD4⁺ T cell subset annotation and bubble diagrams confirm cell identity. **G**, The total CD4⁺ T cell subpopulation frequency varied with the highest Treg (249, 26.7%), Th2 (154, 16.5%), cytotoxic_T (104, 11.1%). **H**, The non-survival group mostly had Treg (33%) and Th2 (23%), whereas the survival group mostly had naive T cells, cytotoxic_T (26%), Treg (10.6%), and Th2 (5%).

Table 4. Single-cell sequencing cell distribution in survivors and non-survivors

	Erythrocyte	Megakaryocyte	B cell	CD14 ⁺ Monocyte	CD16 ⁺ Monocyte	CD16 ⁺ NK	CD56 ⁺ NK	NKT	Cycling T cell	CD8 ⁺ T cell	CD4 ⁺ T cell
S	17	48	2208	597	77	1554	216	649	157	2056	337
N	113	59	51	584	6	356	218	110	263	279	595

N: non-survival group; NK: natural killer; S: survival group.

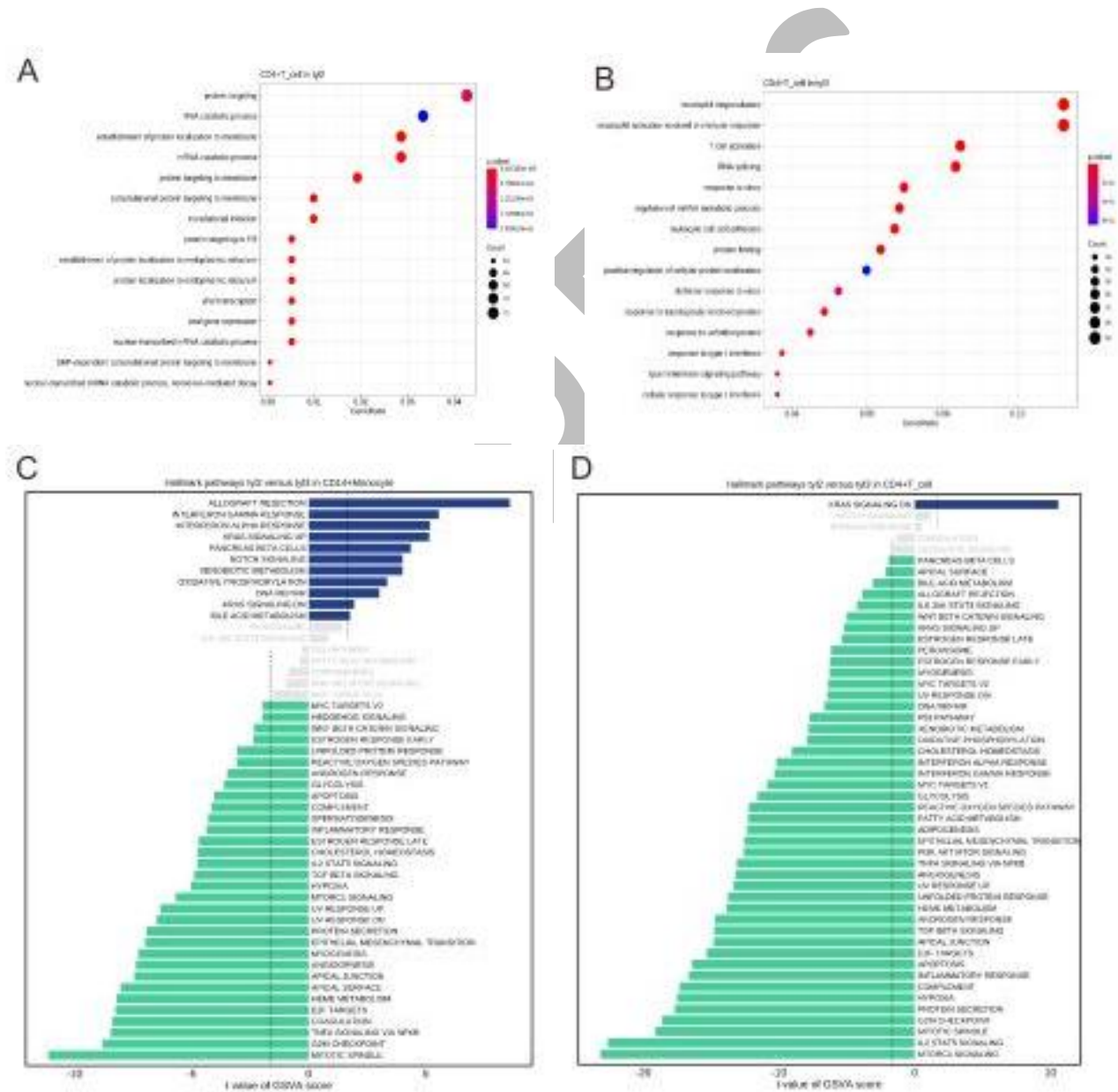


Figure 3. Survival and non-survival gene enrichment analysis. A and B, The Gene Ontology enrichment analyses. B, The non-survival group was dominated by neutrophil degranulation and activation. C and D, The non-survival group expressed more upregulated genes than the survival group in the gene set variation analysis plot.

PJP-ARDS in Immunocompromised Children

The GSVA plot showed that the non-survival group expressed more upregulated genes than the survival group (Figure 3), and that the 5 top gene sets with CD8⁺ T cells were apoptosis, *IL2_STAT5* signaling, mTORC1 signaling, G2M checkpoint, and complement. The top 5 gene sets with the CD4⁺ T cells were mTORC1 signaling, *IL2_STAT5* signaling, mitotic spindle, protein secretion, and hypoxia. The immune status of the non-survival group remained imbalanced, with active immune damage, aggravated apoptosis, leading to CD8⁺ T cell depletion and hypoxic damage. Liu et al found that IL-2 signaling promoted 5-HTP production through the STAT5-TPH1 pathway, leading to the occurrence of CD8⁺ T cell depletion in vitro.¹³ Simultaneously, the expression of genes associated with angiogenesis, epithelial-mesenchymal transition (EMT), inflammatory response, and oxidative stress in CD4⁺ T cells also

increased. These processes may further exacerbate pulmonary inflammatory response and pulmonary fibrosis. The results of GSEA are consistent with those of GSVA.

Cell Communication Analysis

We calculated the significance and signal scores of each ligand-receptor pair and demonstrated the communication of each cell-type-related ligand-receptor pair as a bubble diagram. More signals (*FAS_TNFSF6* (*FASLG*), interferon- γ [IFN- γ], *CD48_CD244*, *CD27_CD70*, *TNFSF10_TNFRSF10* [*TRAIL_Apo2*], *TNFSF14_TNFRSF14*, and *BTLA_TNFRSF14* signals) were expressed in the non-survival group than in the survival group (Figure 4). Genes that were more expressed in the non-survival group included *IL-32*, *S100A*, *LTB*, and tumor necrosis factor (*TNF*).

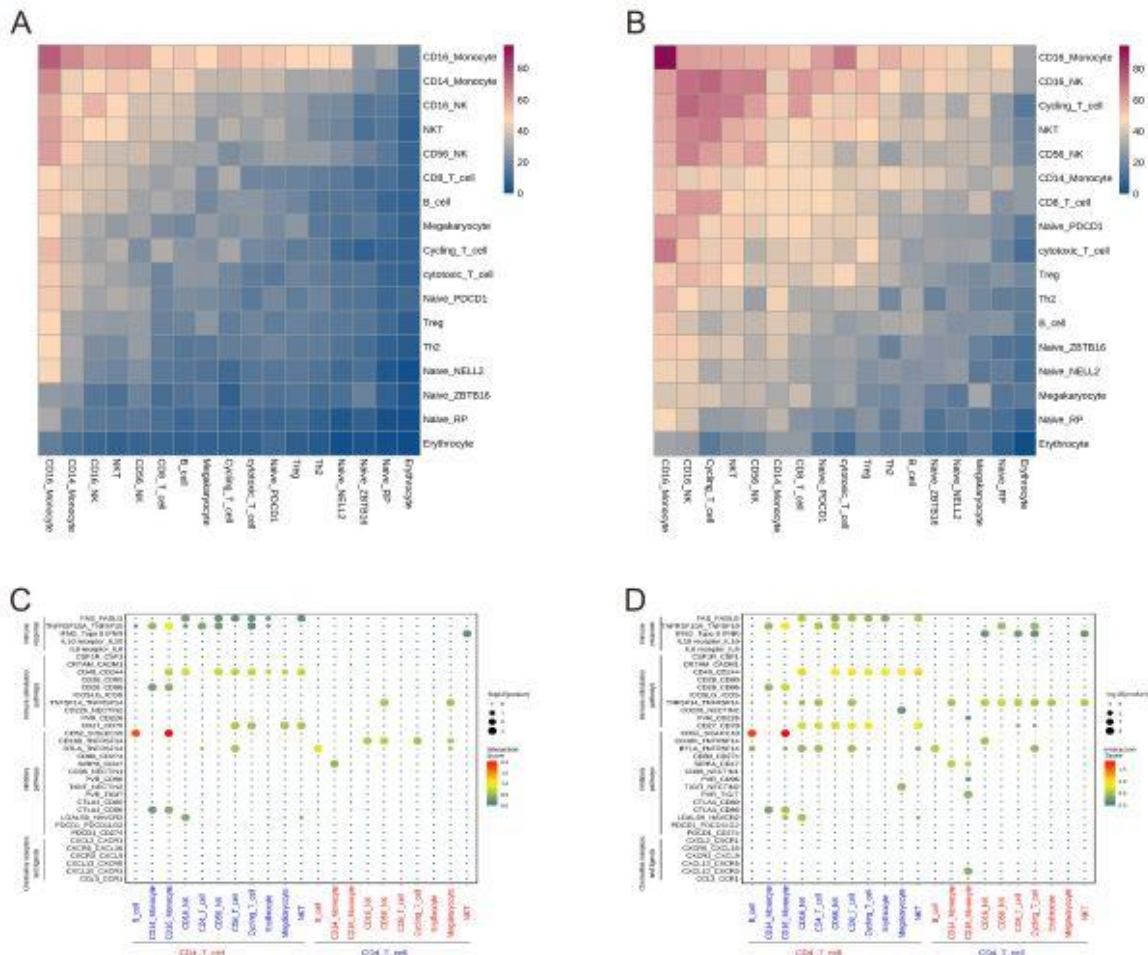


Figure 4. More signals were expressed in the non-survival group than in the survival group. A and B, Heat map showing the correlations between each ligand-receptor pair specific to different cell types. C and D, The bubble chart illustrates the interactions between each of the ligand-receptor pairs associated with different cell types.

T cell number is regulated by proliferation and apoptosis, and fewer CD8⁺ T cells in the non-survival group may be due to increased apoptosis and reduced proliferation rate. *FAS_FASLG*, *TNFSF10*, and *CD27_CD70*, which play a key role in T cell apoptosis, were significantly increased. The Fas/FasL signaling pathway is one of the major regulatory pathways of apoptosis. When Fas function is over-enhanced, CD4⁺ T cells highly express Fas on the surface, and these T cells are susceptible to CTL-mediated cell death.¹⁴ *TNF*-related apoptosis-inducing ligand (TRAIL/APO-2L) is a member of the *TNF* family that promotes apoptosis by binding to the transmembrane receptors TRAIL-R1/DR4 and TRAIL-R2/DR5.¹⁵ *CD27_CD70* maintains T cell homeostasis by activating Fas-driven T cell apoptosis during infection.^{16,17} IFN- γ stimulates T cell-derived CD70 expression and function, whereas APC-expressed CD70 delivers a costimulatory signal by binding to CD27 on T cells. T cell-expressed CD70 plays an unexpected immune checkpoint role that directly restrains T cell responses.¹⁸

Moreover, CD27 can bind to TRAF2 and TRAF3 in addition to *TNF* (all upregulated) and mediate T cell apoptosis in chronic hepatitis C virus-infected individuals. Other proapoptotic genes were upregulated in immune cells of chronic hepatitis C virus-infected patients, inducing spontaneous apoptosis.¹⁹

It seemed that increased levels of inflammation and apoptotic reactions in patients with PJP trigger the potential recruitment of immune exhaustion genes. Furthermore, upregulation of proapoptotic factors functioning via the extrinsic and intrinsic pathways suggests their utility for intracellular fungus persistence, which, however, remains to be investigated.

TNFSF14 (LIGHT) exhibits inflammatory activities in lung fibroblasts complementary to IL-13 and TNF- β , accelerating lung modulation of inflammation and remodeling.²⁰ The *TNFSF14_TNFRSF14* and *BTLA_TNFRSF14* signaling regulatory networks play a regulatory role in various inflammatory, autoimmune, and infectious immune reactions.²¹ In 2012, the HVEM-BTLA signaling pathway was upregulated in the hepatic tissue of patients with chronic hepatitis B virus-related acute-on-chronic liver failure, promoting disease progression.²² In addition, *BTLA* is a crucial molecular marker that promotes the development and progression of sepsis through the inhibition of the innate immune response.²³

In addition to the strong proapoptotic properties, the corresponding elevation of the inflammatory indicators, such as *IL-32*, *S100A*, *LTB*, *TNF*, and IFN- γ , indicated persistent hyperactivity of immune activation. Meanwhile, Supplementary Table S2 provides additional information clarifying the correlations between these transcriptomic findings and the individualized clinical trajectories of the patients. It visually demonstrates the correspondence between immune changes and clinical decisions.

To directly correlate the transcriptomic immune signatures with patient-specific clinical outcomes, we synthesized the key findings into a comprehensive summary (Supplementary Table S3). This table delineates the co-occurrence of distinct immune profiles—specifically, CD8⁺ T cell depletion, elevated Treg ratios with pro-inflammatory features (e.g., high *IL-32* and *S100A* expression), and increased IL-17 levels—with critical clinical parameters, including the timing of anti-PJP therapy initiation and the duration of mechanical ventilation. The visualization explicitly illustrates that a delayed onset of anti-PJP therapy and the emergence of this specific immune dysregulation signature are concurrently associated with non-survival outcomes.

DISCUSSION

Previous studies have identified poor prognostic factors in PJP including advanced age, female sex, diagnostic delays, respiratory failure, solid tumors, elevated lactate dehydrogenase (LDH), hypoalbuminemia, and concurrent bacterial or *Aspergillus* infections.⁸ In two other studies, the overall mortality rate of PJP in HIV-negative patients with respiratory failure was 63%.²⁴ Unsuccessful initial antimicrobial treatment indicates poor prognosis. In our study, the mortality rate of pediatric patients with ARDS with PJP was 25% (5/20). There were no differences in LDH, albumin, or BDG level between the survival and non-survival groups. However, delayed anti-PJP therapy may be a potential risk factor for adverse outcomes.

Given the rarity of pediatric PJP-ARDS, multi-center collaboration is crucial to expand the sample size and validate our findings. We plan to pursue such collaborations in future studies. Furthermore, due to the complex immunopathology and multiple confounding factors involved, more definitive conclusions regarding

pathogenesis and prognosis may require meta-analyses that pool data from multiple studies. This approach can synthesize evidence, mitigate confounding, and enhance the robustness of findings from individual studies with limited sample sizes.

Our findings align with severe inflammatory models like COVID-19, where Treg plasticity and T cell exhaustion drive poor outcomes.²⁵ This highlights shared pathways of immune dysregulation, suggesting that therapeutic strategies might be translatable across diseases to improve pediatric PJP-ARDS management. Specifically, our results confirm that delayed anti-PJP therapy is associated with poorer outcomes, underscoring the critical need for timely empirical treatment in immunocompromised children, a view consistent with other studies.²⁶

The critical role of CD8⁺ T cells in host defense against PJP is increasingly recognized. Tang et al found that a decrease in CD8⁺ T cell count and an increase in the tissue damage marker LDH were the most typical characteristics of patients with PJP.²⁷ Another study also showed that a CD8⁺ T cell count <300/μL was an independent risk factor for death in patients with PJP.²⁸ Our single-cell sequencing results showed that the non-survival group had nearly depleted CD8⁺ T cells. While we infer CD8⁺ T cell exhaustion from this profound depletion and the upregulation of apoptotic pathways (e.g., *FAS*, *FASLG*, *TRAIL*) in our data, it is important to note that our study did not directly assess canonical exhaustion markers such as PD-1, LAG-3, or TIM-3. This constitutes a limitation of the current work. Notably, the relative proportion of Tregs was substantially increased in this context. CD8⁺ T cells are hypothesized to work in conjunction with CD4⁺ T cells to elicit an effective immune response against *Pneumocystis*. de la Rúa et al. found that depletion of CD8⁺ T cells in mice significantly impaired *Pneumocystis* clearance.²⁹ Ruan et al demonstrated that the administration of recombinant human IL-7 to CD4⁺ T cell-depleted mice resulted in an increase in CD8⁺ T cells recruited to the lungs in response to *Pneumocystis* clearance.³⁰ Although CD4⁺ T cells play a central role in coordinating host defenses against *P. jirovecii*, the inhibition and cytotoxic effects of CD8⁺ T cells seem to be critical for controlling and terminating the infection.

According to a recent study comprising patients with severe coronavirus disease 2019 (COVID-19), peripheral Tregs overexpressed a range of suppressive effectors and pro-inflammatory molecules, such as *IL-*

32. Tregs may play various roles in COVID-19 by suppressing anti-viral T cell responses during the severe phase of the disease, and/or via a direct pro-inflammatory role.³¹ This Treg plasticity concept gains support from fungal sepsis studies where Treg-derived *IL-32* drives pathological inflammation,³² as well as from viral pneumonia research that shows *S100A*-mediated Treg polarization toward inflammatory phenotypes.³³ In conditions such as autoimmune diseases and severe infections, Tregs can lose their stable phenotype, transforming into pro-inflammatory “ex-Tregs” that secrete IFN-γ and IL-17.³⁴ The specific upregulation of *IL-32*, as observed in our non-survivors, is particularly noteworthy. *IL-32* is not a typical Treg cytokine; its production marks a significant shift toward a potent pro-inflammatory state, as it directly activates NF-κB and p38 MAPK pathways in neighboring immune and stromal cells, amplifying neutrophil and macrophage-driven tissue injury.³⁵ Similarly, *S100A* proteins, beyond being DAMPs, can autocrinely and paracrinely modulate leukocyte function, including promoting a pro-inflammatory T cell polarization.³⁶ As highlighted in recent reviews, Tregs increasingly demonstrate this dual immunosuppressive and pro-inflammatory functionality in immunocompromised hosts.³⁷ This plasticity is tightly regulated by the microenvironment. In PJP-ARDS, persistent fungal antigen and excessive inflammation (e.g., high IL-17) may drive Tregs toward pro-inflammatory phenotypes, diverging from their classical suppressive role.^{38,39}

We found that Tregs of the non-survival group expressed more *IL-32*, *S100A*, *TNF*, *FAS*, *CD27*, and *IFNGR2*, which may play a pro-inflammatory role rather than a suppressive role. Persistently increased levels of inflammation and apoptotic reactions in patients with PJP result in disordered immune function, which is not conducive to the improvement of the body.

Notably, the overexpression of *IL-32* and *S100A* in Tregs of non-survivors represents a key mechanistic link between immune dysregulation and disease severity. *IL-32*, a potent pro-inflammatory cytokine, amplifies neutrophil recruitment and activation—consistent with our GO enrichment analysis showing neutrophil degranulation as a dominant pathway in non-survivors—exacerbating pulmonary tissue damage.⁴⁰ *S100A* proteins, acting as damage-associated molecular patterns, further fuel inflammation by activating TLR4/NLRP3 signaling, driving cytokine storms and fibrosis in the lungs.⁴¹ Together, these molecules

transform Tregs from immune regulators to pro-inflammatory effectors, creating a pathological loop that impairs pathogen clearance while accelerating lung injury. The co-expression of *IL-32* and *S100A* within Tregs provides a plausible explanation for the simultaneous observation of Treg expansion and uncontrolled inflammation in non-survivors.

To synthesize these complex transcriptomic findings with individual clinical trajectories, we provide a summary table (Supplementary Table S5). This table integrates key immune signatures—profound CD8⁺ T cell depletion, expansion of pro-inflammatory IL-32⁺/S100A⁺ Tregs, and apoptotic pathway activation—with patient-specific timelines, linking them to critical clinical decisions and outcomes.

Clinically, distinguishing this pro-inflammatory Treg phenotype has direct implications for patient management. In immunocompromised hosts, the standard approach might involve reducing immunosuppression to restore immune function. However, our data suggest that in severe PJP-ARDS, a subset of Tregs themselves become drivers of pathology. Therefore, serial immune monitoring aimed at detecting this shift (e.g., through cytokine panels assessing IL-17, *IL-32*) could guide more personalized therapy. Patients with this pro-inflammatory Treg signature might be candidates for adjunctive therapies designed to modulate Treg function or neutralize specific inflammatory mediators like *IL-32*.

These findings highlight the translational potential of targeting Treg plasticity and CD8⁺ T cell survival as adjunctive strategies. The immune signature—CD8⁺ T cell depletion (<100/ μ L), pro-inflammatory IL-32⁺/S100A⁺ Treg expansion, and elevated IL-17—offers a prognostic framework for early risk stratification. Future studies that integrate flow cytometry for direct exhaustion markers (e.g., PD-1, LAG-3, TIM-3) with single-cell sequencing are needed to definitively validate CD8⁺ T cell exhaustion and explore immune checkpoint modulation as a therapeutic strategy. Notably, our GSVA analysis revealed that prolonged mechanical ventilation, more frequently required in non-survivors, may exacerbate disease progression through hypoxia-mediated immune dysregulation. The sustained hypoxic state in these patients appears to activate hypoxia-related pathways (e.g., HIF-1 α signaling) in CD4⁺ T cells,⁴² which may further impair their effector functions while promoting pro-inflammatory polarization. This mechanistic link between iatrogenic

hypoxia (from prolonged ventilation) and T cell dysfunction creates a vicious cycle: hypoxia-induced immune impairment delays *Pneumocystis* clearance, which in turn necessitates continued mechanical support, perpetuating the hypoxic state. These findings suggest that optimizing ventilation strategies to minimize hypoxia while maintaining adequate oxygenation may be crucial for preserving immune function in severe PJP.

Translating this into practice necessitates discussing specific supportive strategies. Beyond standard lung-protective ventilation, advanced modalities like High-Frequency Oscillatory Ventilation (HFOV) or Extracorporeal Membrane Oxygenation (ECMO) may be considered in refractory cases. HFOV minimizes tidal volume swings, potentially reducing ventilator-induced lung injury.⁴³ Venovenous ECMO provides ultimate lung rest, allowing ultra-protective ventilation and potentially mitigating hypoxia-driven immune dysregulation.⁴⁴ The decision to use such supports could be integrated with a patient's immune profile; for instance, a high-risk patient identified by our PJP-ARDS Prognostic Scoring System (PJP-ARDS PSS), showing profound CD8⁺ T cell depletion and a pro-inflammatory Treg signature, might benefit from earlier escalation to these strategies.

Serial monitoring of these markers can guide decisions, such as adjusting immunosuppression when Tregs shift pro-inflammatory. Therapeutically, inhibiting Fas/FasL- or TRAIL-mediated apoptosis (e.g., Fas antagonists) may preserve CD8⁺ T cells, while modulating Tregs to reduce pro-inflammatory cytokines could enhance clearance.^{45,46} These immune interventions, combined with prompt anti-PJP therapy (critical given the impact of treatment delay), may synergistically improve outcomes. Future studies should explore combining early antimicrobials with immunomodulators (e.g., IL-7 to boost CD8⁺ T cells) to break immune dysfunction cycles in pediatric ARDS secondary to PJP.

We propose a PJP-ARDS PSS incorporating key parameters from our cohort (Supplementary Table S4). This conceptual model scores CD8⁺ count (<100/ μ L: 3 points), IL-17 (>20 pg/mL: 2 points), Treg/CD4⁺ ratio (>25%: 2 points), ventilation duration at day 14 (>14 days: 4 points), and anti-PJP therapy delay (>5 days: 2 points). Stratification into Low (0-3), Intermediate (4-6), or High (\geq 7) risk may guide clinical management, with high-risk patients potentially requiring aggressive

immunomodulation. We emphasize that this hypothesis-generating model requires validation in prospective multicenter studies.

There are also some limitations in the present study. Firstly, while CD8⁺ T cell exhaustion was inferred, the lack of direct protein-level assessment of markers like PD-1, LAG-3, or TIM-3 limits our ability to definitively characterize the exhausted phenotype. Second, the relatively small sample size, though representative of this rare pediatric population, necessitates validation in larger multicenter cohorts. Third, and most notably, the single-cell RNA sequencing analysis was performed on only two patients. While this provided high-resolution mechanistic insights, the extremely limited sample size significantly constrains the generalizability of the detailed transcriptomic findings, which must be validated in larger-scale studies. Future research should integrate these markers through flow cytometry to clarify their association with CD8⁺ T cell exhaustion, thereby potentially identifying immune checkpoint targets to reverse the cell exhaustion phenomenon in severe PJP. Additionally, given the complexity of PJP pathogenesis and confounding variables, future work should prioritize meta-analyses to pool results from independent studies, which will help overcome the limitations of small sample sizes and generate more definitive conclusions.

STATEMENT OF ETHICS

All procedures performed in this study involving human participants were in accordance with the ethical standards of the institutional and/or national research committee and with the 1964 Helsinki Declaration and its later amendments or comparable ethical standards. The study was approved by The First Affiliated Hospital, Sun Yat-sen University (No.201306ZS50).

FUNDING

Not applicable.

CONFLICT OF INTEREST

The authors declare no conflicts of interest.

ACKNOWLEDGMENTS

Not applicable.

DATA AVAILABILITY

Data is available from the corresponding author on request.

AI ASSISTANCE DISCLOSURE

No artificial intelligence (AI) tools were used.

REFERENCES

1. Morris A, Lundgren JD, Masur H, Walzer PD, Hanson DL, Frederick T, et al. Current epidemiology of Pneumocystis pneumonia. *Emerg Infect Dis*. 2004;10(10):1713-20.
2. Matsumura Y, Shindo Y, Iinuma Y, Yamamoto M, Shirano M, Matsushima A, et al. Clinical characteristics of Pneumocystis pneumonia in non-HIV patients and prognostic factors including microbiological genotypes. *BMC Infect Dis*. 2011;11:76.
3. Tasaka S, Tokuda H. Pneumocystis jirovecii pneumonia in non-HIV-infected patients in the era of novel immunosuppressive therapies. *J Infect Chemother*. 2012;18(6):793-806.
4. Monnet X, Vidal-Petiot E, Osman D, Hamzaoui O, Durrbach A, Goujard C, et al. Critical care management and outcome of severe Pneumocystis pneumonia in patients with and without HIV infection. *Crit Care*. 2008;12(1):R28.
5. Ko Y, Jeong BH, Park HY, Koh WJ, Suh GY, Chung MP, et al. Outcomes of Pneumocystis pneumonia with respiratory failure in HIV-negative patients. *J Crit Care*. 2014;29(3):356-61.
6. Alvarez-Martinez MJ, Miró JM, Valls ME, Moreno A, Rivas PV, Solé M, et al. Sensitivity and specificity of nested and real-time PCR for the detection of Pneumocystis jirovecii in clinical specimens. *Diagn Microbiol Infect Dis*. 2006;56(2):153-60.
7. Fan LC, Lu HW, Cheng KB, Li HP, Xu JF. Evaluation of PCR in bronchoalveolar lavage fluid for diagnosis of Pneumocystis jirovecii pneumonia: a bivariate meta-analysis and systematic review. *PLoS One*. 2013;8(9):e73099.
8. Liu Y, Su L, Jiang SJ, Qu H. Risk factors for mortality from pneumocystis carinii pneumonia (PCP) in non-HIV patients: a meta-analysis. *Oncotarget*. 2017;8(35):59729-39.
9. Roblot F, Godet C, Le Moal G, Garo B, Faouzi Souala M, Dary M, et al. Analysis of underlying diseases and

- prognosis factors associated with *Pneumocystis carinii* pneumonia in immunocompromised HIV-negative patients. *Eur J Clin Microbiol Infect Dis*. 2002;21(7):523-31.
10. Gaborit BJ, Tessoulin B, Lavergne RA, Morio F, Sagan C, Canet E, et al. Outcome and prognostic factors of *Pneumocystis jirovecii* pneumonia in immunocompromised adults: a prospective observational study. *Ann Intensive Care*. 2019;9(1):131.
 11. Fujii T, Nakamura T, Iwamoto A. *Pneumocystis pneumonia* in patients with HIV infection: clinical manifestations, laboratory findings, and radiological features. *J Infect Chemother*. 2007;13(1):1-7.
 12. Cereser L, Dallorto A, Candoni A, Volpetti S, Righi E, Zuiani C, et al. *Pneumocystis jirovecii* pneumonia at chest High-resolution Computed Tomography (HRCT) in non-HIV immunocompromised patients: Spectrum of findings and mimickers. *Eur J Radiol*. 2019;116:116-27.
 13. Liu Y, Zhou N, Zhou L, Wang J, Zhou Y, Zhang T, et al. IL-2 regulates tumor-reactive CD8(+) T cell exhaustion by activating the aryl hydrocarbon receptor. *Nat Immunol*. 2021;22(3):358-69.
 14. Li S, Zhao Y, He X, Kim TH, Kuharsky DK, Rabinowich H, et al. Relief of extrinsic pathway inhibition by the Bid-dependent mitochondrial release of Smac in Fas-mediated hepatocyte apoptosis. *J Biol Chem*. 2002;277(30):26912-20.
 15. Lavrik IN. Systems biology of death receptor networks: live and let die. *Cell Death Dis*. 2014;5(5):e1259.
 16. Watts TH. TNF/TNFR family members in costimulation of T cell responses. *Annu Rev Immunol*. 2005;23:23-68.
 17. Wensveen FM, Unger PP, Kragten NA, Derks IA, ten Brinke A, Arens R, et al. CD70-driven costimulation induces survival or Fas-mediated apoptosis of T cells depending on antigenic load. *J Immunol*. 2012;188(9):4256-67.
 18. O'Neill RE, Du W, Mohammadpour H, Alqassim E, Qiu J, Chen G, et al. T Cell-Derived CD70 Delivers an Immune Checkpoint Function in Inflammatory T Cell Responses. *J Immunol*. 2017;199(10):3700-10.
 19. Barathan M, Gopal K, Mohamed R, Ellegård R, Saeidi A, Vadivelu J, et al. Chronic hepatitis C virus infection triggers spontaneous differential expression of biosignatures associated with T cell exhaustion and apoptosis signaling in peripheral blood mononucleocytes. *Apoptosis*. 2015;20(4):466-80.
 20. da Silva Antunes R, Mehta AK, Madge L, Tocker J, Croft M. TNFSF14 (LIGHT) Exhibits Inflammatory Activities in Lung Fibroblasts Complementary to IL-13 and TGF- β . *Front Immunol*. 2018;9:576.
 21. Shui JW, Steinberg MW, Kronenberg M. Regulation of inflammation, autoimmunity, and infection immunity by HVEM-BTLA signaling. *J Leukoc Biol*. 2011;89(4):517-23.
 22. Xu H, Cao D, Guo G, Ruan Z, Wu Y, Chen Y. The intrahepatic expression and distribution of BTLA and its ligand HVEM in patients with HBV-related acute-on-chronic liver failure. *Diagn Pathol*. 2012;7:142.
 23. Shubin NJ, Chung CS, Heffernan DS, Irwin LR, Monaghan SF, Ayala A. BTLA expression contributes to septic morbidity and mortality by inducing innate inflammatory cell dysfunction. *J Leukoc Biol*. 2012;92(3):593-603.
 24. Boonsangskuk V, Sirilak S, Kiatboonsri S. Acute respiratory failure due to *Pneumocystis pneumonia*: outcome and prognostic factors. *Int J Infect Dis*. 2009;13(1):59-66.
 25. Dhawan M, Rabaan AA, Alwarthan S, Alhajri M, Halwani MA, Alshengeti A, et al. Regulatory T Cells (Tregs) and COVID-19: Unveiling the Mechanisms, and Therapeutic Potentialities with a Special Focus on Long COVID. *Vaccines*. 2023.
 26. Poddighe D. *Mycoplasma pneumoniae*-related extrapulmonary diseases and antimicrobial therapy. *Journal of Microbiology, Immunology and Infection*. 2019.
 27. Tang G, Tong S, Yuan X, Lin Q, Luo Y, Song H, et al. Using Routine Laboratory Markers and Immunological Indicators for Predicting *Pneumocystis jirovecii* Pneumonia in Immunocompromised Patients. *Front Immunol*. 2021;12:652383.
 28. Jin F, Xie J, Wang HL. Lymphocyte subset analysis to evaluate the prognosis of HIV-negative patients with *pneumocystis pneumonia*. *BMC Infect Dis*. 2021;21(1):441.
 29. de la Rúa NM, Samuelson DR, Charles TP, Welsh DA, Shellito JE. CD4(+) T-Cell-Independent Secondary Immune Responses to *Pneumocystis Pneumonia*. *Front Immunol*. 2016;7:178.
 30. Ruan S, Samuelson DR, Assouline B, Morre M, Shellito JE. Treatment with Interleukin-7 Restores Host Defense against *Pneumocystis* in CD4+ T-Lymphocyte-Depleted Mice. *Infect Immun*. 2016;84(1):108-19.
 31. Galván-Peña S, Leon J, Chowdhary K, Michelson DA, Vijaykumar B, Yang L, et al. Profound Treg perturbations correlate with COVID-19 severity. *Proc Natl Acad Sci U S A*. 2021;118(37).

PJP-ARDS in Immunocompromised Children

32. Zhu G, Liao Y, Liu S, Liu P, Yang K, Tan M, et al. Dysregulated Immune Responses in Sepsis: Insights From Treg-Related Gene Expression. *Journal of Inflammation Research*. 2025.
33. Ostermann L, Seeliger B, David S, Flasche C, Maus R, Reinboth MS, et al. S100A9 is indispensable for survival of pneumococcal pneumonia in mice. *PLoS Pathogens*. 2023.
34. Ortega-Mejia II, Romero-López N, Casasola-Vargas JC, Burgos-Vargas R, Domínguez-López ML, Romero-López JP. Treg cell plasticity as a driver of inflammation in spondyloarthritis and psoriasis. *Frontiers in Immunology*. 2025.
35. Jo H, Shin S, Agura T, Jeong S, Ahn H, Lee J, et al. The Role of α -Enolase on the Production of Interleukin (IL)-32 in Con A-Mediated Inflammation and Rheumatoid Arthritis (RA). *Pharmaceuticals*. 2024.
36. Schenten V, Plançon S, Jung N, Hann J, Bueb J-L, Bréchar S, et al. Secretion of the Phosphorylated Form of S100A9 from Neutrophils Is Essential for the Proinflammatory Functions of Extracellular S100A8/A9. *Frontiers in Immunology*. 2018.
37. Liu J, Zhang B, Zhang G, Shang D. Reprogramming of regulatory T cells in inflammatory tumor microenvironment: can it become immunotherapy turning point? *Frontiers in Immunology*. 2024.
38. Xing Y, Hogquist KA. T-cell tolerance: central and peripheral. *Cold Spring Harb Perspect Biol*. 2012;4(6).
39. Maessen L, Boers LS, Heylen J, van Someren Gréve F, Wauters J, Bos LDJ, et al. Viral reactivations and fungal infections in nonresolving acute respiratory distress syndrome. *European Respiratory Review*. 2025.
40. Zhang J, Sun X, Zhong L, Shen B. IL-32 exacerbates adenoid hypertrophy via activating NLRP3-mediated cell pyroptosis, which promotes inflammation. *Molecular Medicine Reports*. 2021.
41. Hiroshima Y, Hsu K, Tedla N, Wong SW, Chow S, Kawaguchi N, et al. S100A8/A9 and S100A9 reduce acute lung injury. *Immunology and Cell Biology*. 2017.
42. Zhuang H, Zhang Z, Chen B, Tang C, Chen X, Tan W, et al. Prognostic stratification based on HIF-1 α signaling for evaluating hypoxia status and immune landscape in hepatocellular carcinoma. *Journal of Big Data*. 2023.
43. Klapsing P, Moerer O, Wende C, Herrmann P, Quintel M, Bleckmann A, et al. High-frequency oscillatory ventilation guided by transpulmonary pressure in acute respiratory syndrome: an experimental study in pigs. *Critical Care*. 2018.
44. Song L, Li K, Hong X, Xiao K, Mo G, Zheng M, et al. Transcriptomic evidence of lung repair in paediatric ARDS survival. *Clinical and Translational Medicine*. 2023.
45. Hua S, Gu X, Jin H, Zhang X, Liu Q, Yang J. Tumor-infiltrating T lymphocytes: A promising immunotherapeutic target for preventing immune escape in cholangiocarcinoma. *Biomedicine & Pharmacotherapy*. 2024.
46. Upadhyay R, Boiarsky JA, Pantsulaia G, Svensson-Arvelund J, Lin MJ, Wroblewska A, et al. A Critical Role for Fas-Mediated Off-Target Tumor Killing in T-cell Immunotherapy. *Cancer Discovery*. 2021.